Next Generation QTAIM for the Design of Quinone-based Switches

Tian Tian[1], Tianlv Xu[1], Lingling Wang[1], Yang Ping [1], Tanja van Mourik[2], Herbert Früchtl[2], Steven R. Kirk[*1] and Samantha Jenkins[*1]

[1]Key Laboratory of Chemical Biology and Traditional Chinese Medicine Research and Key Laboratory of Resource Fine-Processing and Advanced Materials of Hunan Province of MOE, College of Chemistry and Chemical Engineering, Hunan Normal University, Changsha, Hunan 410081, China

[2]EaStCHEM School of Chemistry, University of St Andrews, North Haugh, St Andrews, Fife KY16 9ST, Scotland, United Kingdom.

*email: samanthajsuman@gmail.com

*email:steven.kirk@cantab.net

1. Supplementary Materials S1. The variation of the metallicity $\xi(\mathbf{r}_b)$ with the IRC for N10--H13 *BCP* and N11--H13 *BCP*.

2. Supplementary Materials S2. The QTAIM, bond-path framework set $\mathsf{B} = \{\boldsymbol{p},\boldsymbol{q},\boldsymbol{r}\}$.

3. Supplementary Materials S3. The complete set of **{*q*,*q'*}-**paths for the quinone switch.

4. Supplementary Materials S4. The complete set of **{*p*,*p'*}-**paths for the quinone switch.

1. Supplementary Materials S1.

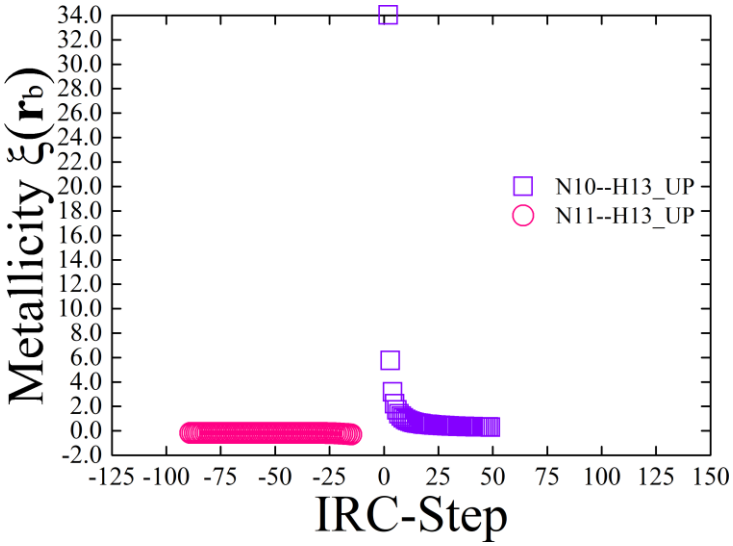

(a)

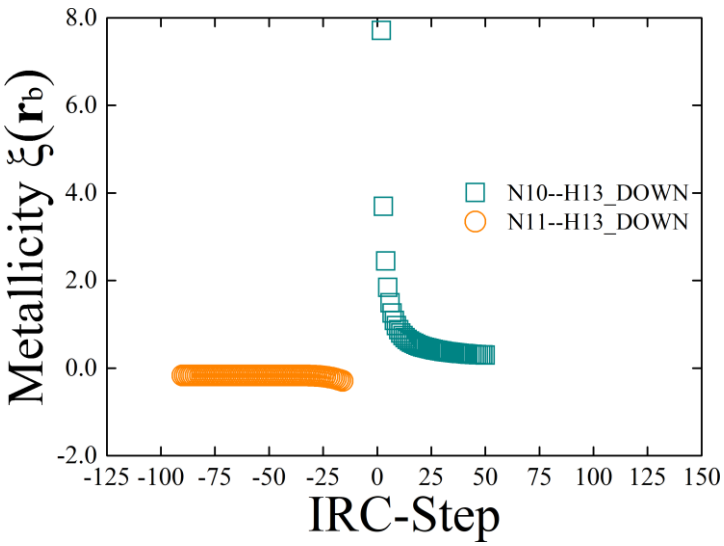

(b)

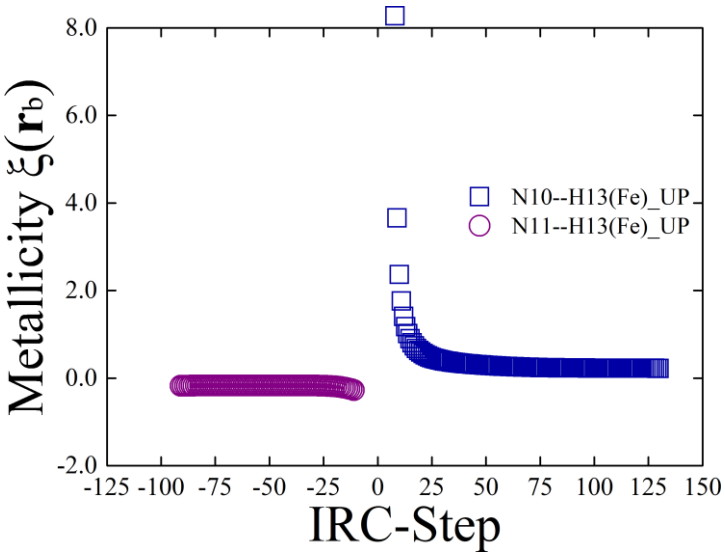

(c)

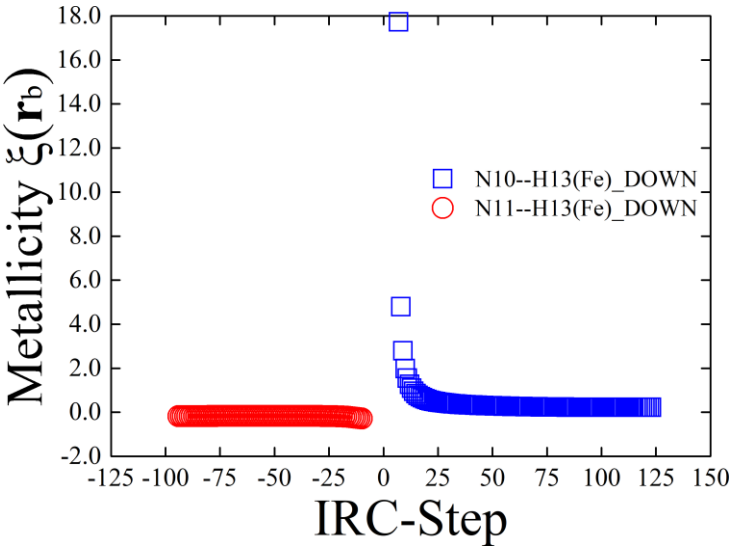

(d)

Figure S1. The variation of the metallicity $\xi(\mathbf{r}_b)$ with the IRC for N10--H13 *BCP* and N11--H13 *BCP* of the F-decorated quinone switch without and with are presented in sub-figures **(a-d)**, respectively.

2. Supplementary Materials S2

With n scaled eigenvector $\underline{\mathbf{e}}_2$ tip path points on the $\boldsymbol{q}$-path where ε_i = ellipticity at the i^{th} bond-path point $\boldsymbol{r}_i$ on the bond-path $\boldsymbol{r}$. It should be noted that the bond-path $\boldsymbol{r}$ is associated with the λ_3 eigenvalues of the $\underline{\mathbf{e}}_3$ eigenvector does not take into account differences in the λ_1 and λ_2 eigenvalues of the $\underline{\mathbf{e}}_1$ and $\underline{\mathbf{e}}_2$ eigenvectors. Analogously, for the $\underline{\mathbf{e}}_1$ tip path points on the $\boldsymbol{p}$-path where ε_i = ellipticity at the i^{th} bond-path point $\boldsymbol{r}_i$ on the bond-path $\boldsymbol{r}$, where the $\boldsymbol{p}_i$ and $\boldsymbol{q}_i$ are defined by:

$$\boldsymbol{p}_i = \boldsymbol{r}_i + \varepsilon_i \mathbf{e}_{1,i} \qquad \textbf{(3a)}$$

$$\boldsymbol{q}_i = \boldsymbol{r}_i + \varepsilon_i \mathbf{e}_{2,i} \qquad \textbf{(3b)}$$

We referred to the next-generation QTAIM interpretation of the chemical bond as the *bond-path framework set*, denoted by B, where $\mathsf{B} = \{\boldsymbol{p},\boldsymbol{q},\boldsymbol{r}\}$ with the consequence that for the ground state a bond is comprised of three 'linkages'; ***p***-, ***q***- and ***r***-paths associated with the $\underline{\mathbf{e}}_1$, $\underline{\mathbf{e}}_2$ and $\underline{\mathbf{e}}_3$ eigenvectors, respectively.

The $\boldsymbol{p}$ and $\boldsymbol{q}$ parameters define eigenvector-following paths with lengths H^* and H, see **Scheme 2**:

$$\mathbb{H}^* = \sum_{i=1}^{n-1} |\boldsymbol{p}_{i+1} - \boldsymbol{p}_i| \qquad \textbf{(4a)}$$

$$\mathbb{H} = \sum_{i=1}^{n-1} |\boldsymbol{q}_{i+1} - \boldsymbol{q}_i| \qquad \textbf{(4b)}$$

The lengths of the *eigenvector-following paths* H^* or H refers to the fact that the tips of the scaled $\underline{\mathbf{e}}_1$ or $\underline{\mathbf{e}}_2$ eigenvectors sweep out along the extent of the bond-path, defined by the $\underline{\mathbf{e}}_3$ eigenvector, between two bonded nuclei connected by a bond-path. In the limit of vanishing ellipticity $\varepsilon = 0$, *for all* steps i along the bond-path then H = BPL.

From equation **(3a)** and equation **(3b)** we see for shared-shell *BCP*s, in the limit of the ellipticity $\varepsilon \approx 0$ i.e. corresponding to single bonds, we then have $\boldsymbol{p}_i = \boldsymbol{q}_i = \boldsymbol{r}_i$ and therefore the value of the lengths H^* and H attain their lowest limit; the bond-path length (r) BPL. Conversely, higher values of the ellipticity ε, for instance, corresponding to double bonds will always result in values of H^* and $\mathsf{H} >$ BPL.

Analogous to the bond-path curvature, see equation **(2)**, we may define dimensionless, *fractional* versions of the eigenvector-following path with length H where several forms are possible and not limited to the following:

$$\mathbb{H}_f = (\mathbb{H} - \mathrm{BPL})/\mathrm{BPL} \qquad \textbf{(5)}$$

A similar expressions to equation (**5**) for H^*_f can be derived using the $\underline{\mathbf{e}}_1$ eigenvector.

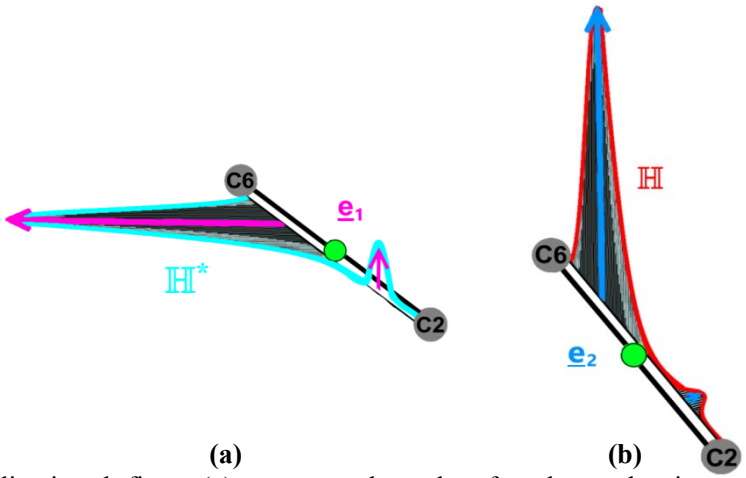

(a) **(b)**

Figure S1. The pale-blue line in sub-figure **(a)** represents the path, referred to as the eigenvector-following path with length H^*, swept out by the tips of the scaled $\underline{\mathbf{e}}_1$ eigenvectors, shown in magenta, and defined by equation **(4a)**. The red path in sub-figure **(b)** corresponds to H, constructed from the path swept out by the tips of the scaled $\underline{\mathbf{e}}_2$ eigenvectors, shown in mid-blue and is defined by equation **(4b)**. The pale-blue and mid-blue arrows representing the $\underline{\mathbf{e}}_1$ and $\underline{\mathbf{e}}_2$ eigenvectors are scaled by the ellipticity ε respectively, where the vertical scales are exaggerated for visualization purposes. The green sphere indicates the position of a given *BCP*.

3. Supplementary Materials S3.

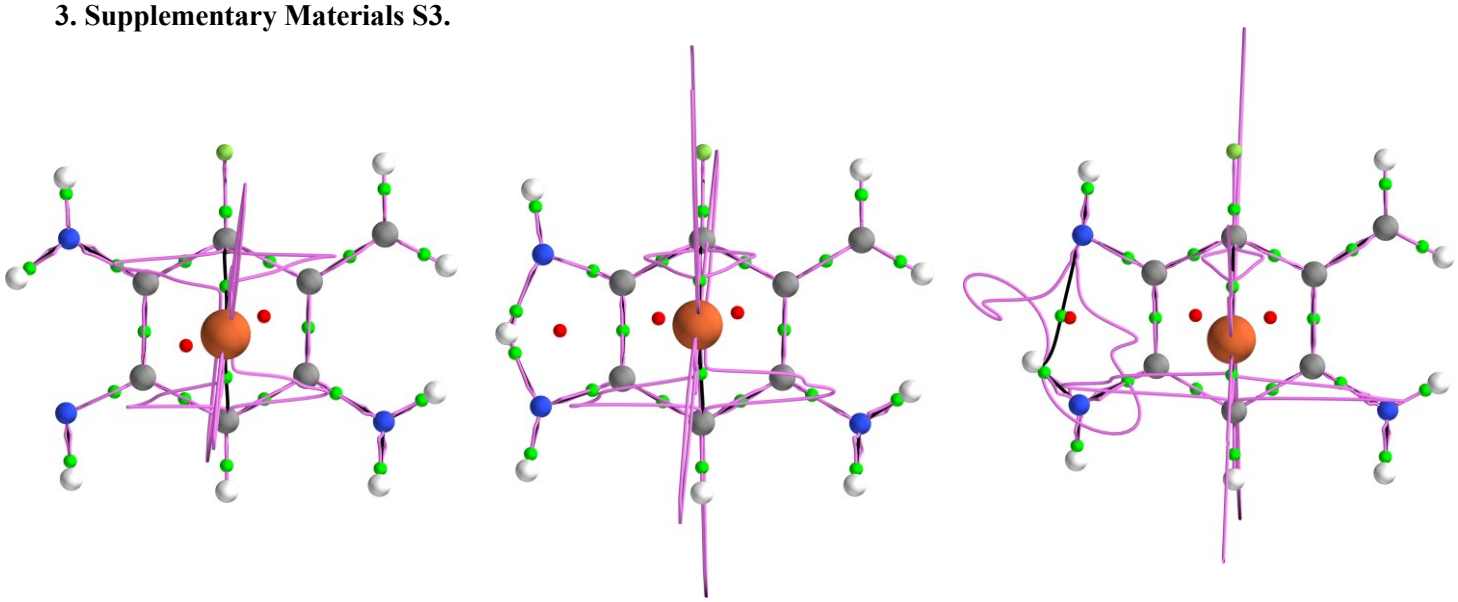

(a)

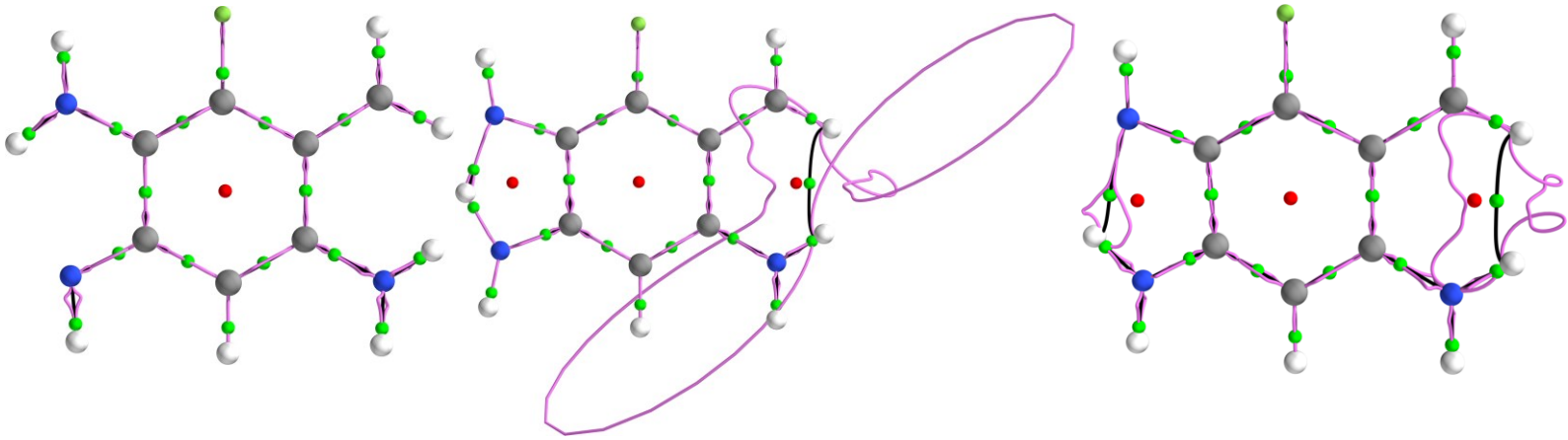

(b)

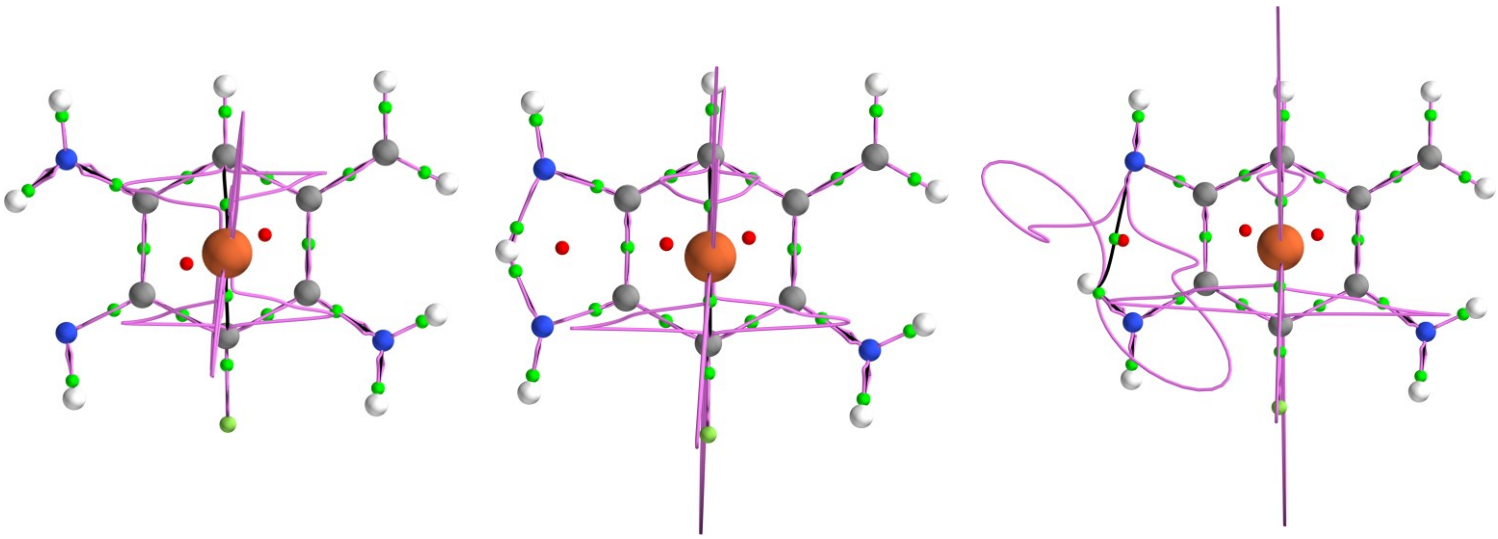

(c)

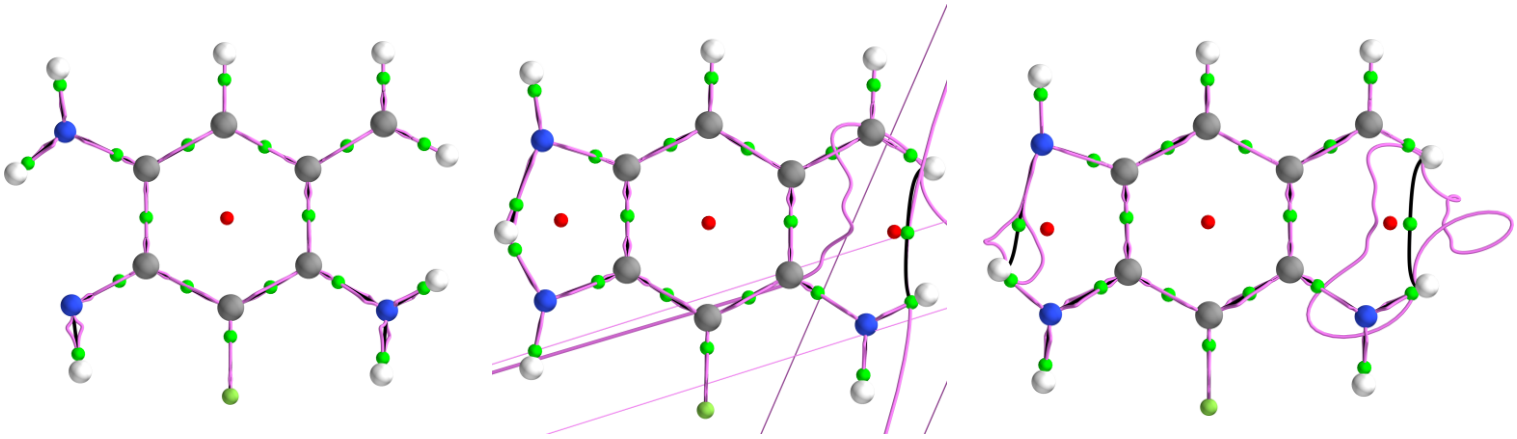

(d)

Figure S3. The {***q,q'***}-paths of the quinone switch doped and undoped with Fe with F(UP) decorated is shown in sub-figures **(a-b)** respectively and F(DOWN) in sub-figures **(c-d)** respectively. The undecorated green and red spheres indicate the positions of the bond critical points (*BCP*s) and ring critical points (*RCP*), see also **Scheme 1** for the atom numbering scheme.

4. Supplementary Materials S4.

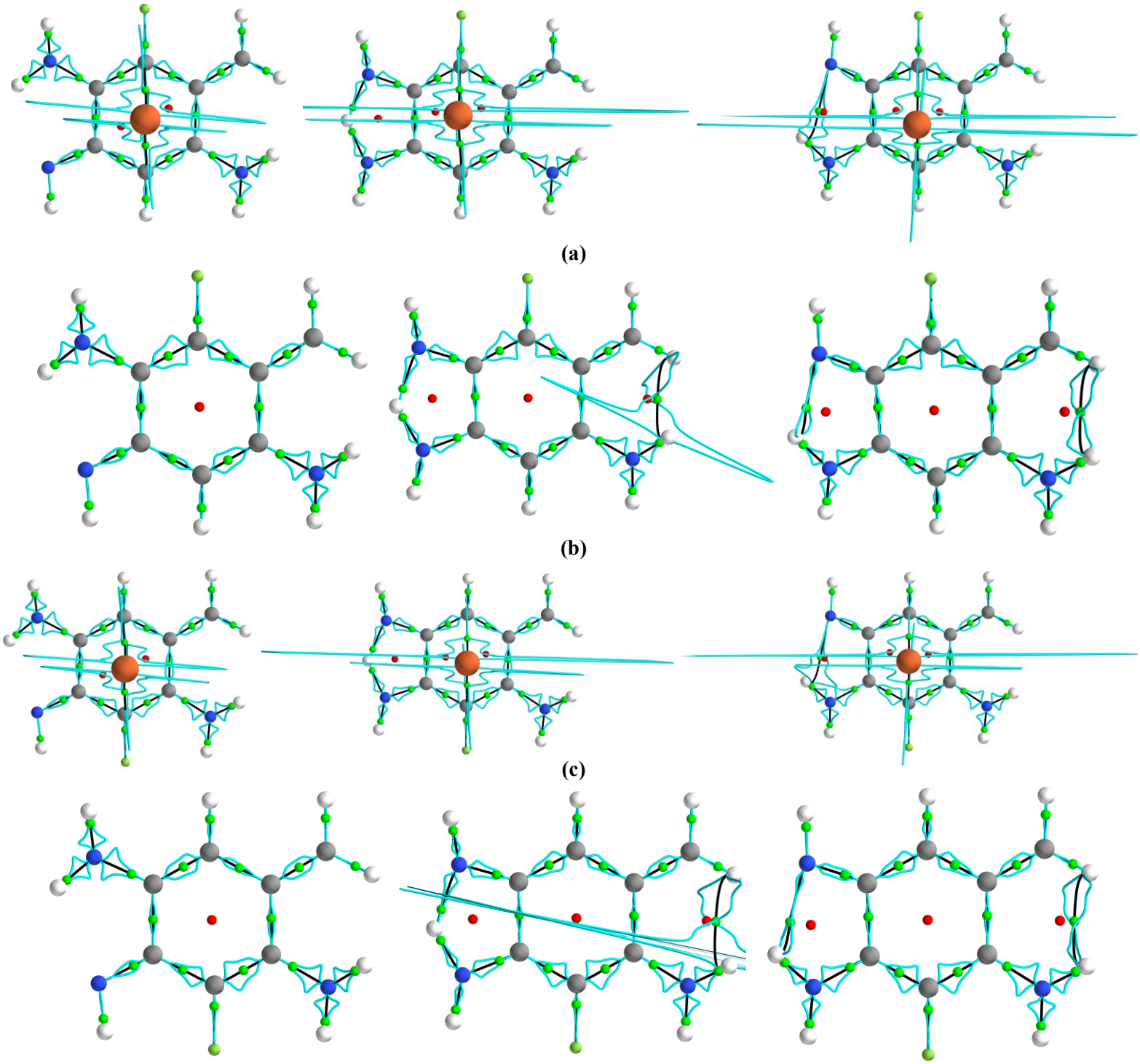

Figure S4. The {***p,p'***}-paths of the quinone switch doped and undoped with Fe with F(UP) decorated is shown in sub-figures **(a-b)** and F(DOWN) in sub-figures **(c-d)**. The see the captions of **Figure S3** and **Figure 1** for further details.